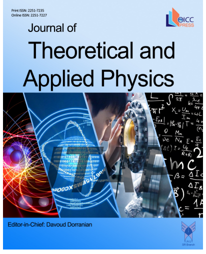

Volume 18, Issue 3, 182444 (1-6)

Journal of Theoretical and Applied Physics (JTAP)

https://dx.doi.org/10.57647/j.jtap.2024.1803.44

Effect of pre-bunched relativistic electron beams on the output power in a two-stream free electron laser

Nader Mahdizadeh[1]*, Maryam Razaghzadeh[2], Alireza Haghpeima[2], Babak Haghighi[2]

[1]*Department of Physics, Sabzevar Branch, Islamic Azad University, Sabzevar, Iran.*
[2]*Department of Physics, Mashhad Branch, Islamic Azad University, Mashhad, Iran.*

*__Corresponding author:__ mahdizadeh@iaus.ac.ir

Original Research

Received:
2 February 2024
Revised:
18 March 2024
Accepted:
3 April 2024
Published online:
25 May 2024

Abstract:

We investigate the effect of pre-bunched relativistic electron beams on the output power of a free electron laser by two electron beams in a theoretical study. In general, this highly coherent and stable pulse of laser is known as the best investigator of basic importance for present-day science. Free electron lasers are the best candidates for exploring nature at ultrasmall spatial and ultrafast temporal scales. In this paper, we have considered the distribution function of relativistic electron beams as a water-bag, and the configuration of the wiggler pump has assumed a helical magneto-static wiggler. By a set of nonlinear, 1D, coupled differential equations the wave-particle interaction problem has been analyzed. With the aid of MATLAB-based Runge-Kutta algorithm numerical solution has been obtained. Saturation profiles in different cases of pre-bunching phase region of beams have been plotted. Out-coming has shown that the saturation length decreases by about 7.2%. However, the amplitude of the output pulse increased by about 209.3% in comparison to the non-pre-bunched relativistic electron beams.

Keywords: Free electron laser; Pre-bunching; Relativistic electron beams; Two-stream; Water-bag distribution function; Wave-particle interaction; Momentum and Maxwell equations

1. Introduction

Free-electron laser (FEL) is a promising high-frequency radiation source, in which a relativistic electron beam (REB) is propagated through an active medium (magneto-static or electromagnetic wiggler) with/without a laser beam as an input seed radiation. In seeded FELs mode, an electromagnetic wave (EMW) is provided by an external laser. However, in self-amplified spontaneous emission (SASE) mode, the EMW is provided by spontaneous incoherent emission. In both modes, the necessary condition for lase is "phase matching" of EMW and plasma waves [1]. When the resonance occurs, energy can be transferred from the REBs into the radiation (known as amplifiers; FELs). While the REBs are co-propagating with the EMW in the wiggler, their energy is modulated with a wavelength of the EMW. Further propagation through the wiggler, energy modulation causes the spatial modulation of the EEBs densities. Thereby, the REBs are being micro-bunched which generates a coherent emission at the main wavelength. Nevertheless, some interesting schemes from the considered model have been proposed by researchers to produce radiation in terahertz [2–11] as well as soft and hard X-ray [12, 13] bands with laser-like properties. In recent modern FELs, the generation of femtosecond pulses with gigawatt peak power and output wavelengths band from several tens of nanometers to 0.1 nm is routine, [14] (and references therein).

The rationale of great interest to FELs is due to their unique features, such as high resolution, tunability, and high efficiency [12]. The special benefits of FELs are to increase their application from plasma heating in electron cyclotron resonance for nuclear fusion to long-range radars, biomedical, photochemistry, isotope separation, material polishing, physical research, as well as in the military [13, 14]. The breakthrough progresses are achieved in seeded FELs, which are the so-called 'pre-bunching' technique. It is a way to produce tunable, Fourier-transform-limited, X-ray

pulses, that is an important prob for present-day basic sciences, like chemistry, biology, and physics [15].
Higher efficiency is achievable by installing the beam-buncher before the main wiggler. Saldin and his coworkers have shown, that the using of the pre-buncher increases the efficiency of the common FEL radiation by a factor of 2 [1]. Emma et al. have verified high-efficiency tapered FELs with a pre-bunched electron beam [16]. In an experimental work at longer wavelengths of seeded FELs mode, 30% energy extraction in a strongly tapered wiggler from a pre-bunched electron beam was reported [17]. Using 1D simulation they have derived the scaling laws. The effect of beam pre-bunching on saturation characteristics of Raman FEL with a helical wiggler and an axial magnetic field has been done in Ref. [18]. In the framework of nonlocal theory, Bhasin and Sharma have investigated the effect of beam pre-bunching on the gain and efficiency [19]. The effect of the pre-bunched electron beam on the laser length in oscillation mode, by 1D simulation has been investigated in Ref. [20]. A review of electron beam bunching methods has been presented by Bessonov [21].
Nonetheless, all of these research works that listed above have been done in FELs with one REB. In this contribution, we have investigated the pre-bunching effects on some characteristics in a model of FELs with two REBs. The idea of using two REBs in FELs rather than one was originally proposed by Bekefi and Jacobs [22], in which two-stream instability plays an essential role in increasing the gain and peak growth rate. Extensive theoretical works have been done on two-stream FELs to do so [23–28] and references therein. For example, more recently Mirian et al. have verified the effect of REB temperature on FEL characteristics with pre-bunched two REBs [27]. However, their study was devoted to a planar wiggler pump and Gaussian distribution function for REBs. Here, we have considered a helical wiggler pump and a water-bag distribution function for REBs. However, this work is in line with our previous works [28–30], but it is new and has not been reported yet.
The paper is organized as follows. First, the governing equations are introduced. Subsequently, by using a fast MATLAB-based 1D two-stream FEL code [31], numerical solutions are presented. The final section is devoted to the results.

2. Governing equations

Suppose two REBs with almost different velocities propagate in one direction (z-direction) through a helical magnetostatic pump according to the following equation

$$\mathbf{B}(z) = B_w[\hat{e}_x \cos(k_w z) + \hat{e}_y \sin(k_w z)]. \tag{1}$$

where B_w, $k_w = 2\pi/\lambda_w$, λ_w and $\hat{e}_x$, $\hat{e}_y$, $\hat{e}_z$ are the amplitude of the wiggler field, the wiggler wave number, wiggler wavelength, and the unit vectors of a Cartesian coordinate system, respectively. It is convenient, instead of the fluctuating electromagnetic fields the vector and scalar potentials in the Coulomb gauge be used, which can be written as [12, 30, 31]

$$\delta\mathbf{A}(z,t) = \delta\hat{A}(z)[\cos\alpha_+(z,t)\hat{e}_x - \sin\alpha_+(z,t)\hat{e}_y], \tag{2}$$

and

$$\delta\varphi(z,t) = \delta\hat{\varphi}(z)\cos\alpha(z,t). \tag{3}$$

Here, z and t refer to the axial distance and entrance time. The phase of the EMW of frequency ω and wavenumber k_+ is given by

$$\alpha_+(z,t) = \int_0^z d\acute{z}k_+(\acute{z}) - \omega t, \tag{4}$$

and

$$\alpha(z,t) = \int_0^z d\acute{z}k(\acute{z}) - \omega t \tag{5}$$

is the phase of the space-charge wave with the same frequency ω and the wave number k. It is assumed implicitly that the amplitudes and wave numbers vary slowly over a wavelength which is known as slow time scale formalism. To derive the dynamical equations which, govern the evolution of the radiation, the scalar and vector potentials of radiation and space-charge wave are substituted into Maxwell's equations. In the Coulomb gauge, the Maxwell equations result in a set of first-order differential equations for δa, Γ_+, $\bar{k}_+$, and $\delta\varphi$ read [12, 30, 31]

$$\frac{d\delta a}{d\bar{z}} \equiv \Gamma_+\delta a, \tag{6a}$$

$$\begin{aligned}\frac{d\Gamma_+}{d\bar{z}} =&(-\bar{\omega}^2 + \bar{k}_+^2 - \Gamma_+^2) + \\ &\Sigma_{i=1}^2 \frac{\omega_{bi}^2\beta_{z0i}}{\delta a}\langle\frac{u_{1i}\cos\psi_i - u_{2i}\sin\psi_i}{|u_{3i}|}\rangle\end{aligned} \tag{6b}$$

$$\frac{d\bar{k}_+}{d\bar{z}} = -2\bar{k}_+\Gamma_+ - \Sigma_{i=1}^2 \frac{\omega_{bi}^2\beta_{z0i}}{\delta a}\langle\frac{u_{1i}\sin\psi_i - u_{2i}\cos\psi_i}{|u_{3i}|}\rangle, \tag{6c}$$

$$\frac{d\delta\varphi}{d\bar{z}} = -2\Sigma_{i=1}^2 \frac{\omega_{bi}^2}{\delta a\bar{\omega}}\langle\sin\psi_{sci}\rangle \tag{6d}$$

where $\mathbf{u}_i = \mathbf{p}_i/mc$ and $\mathbf{p}_i$ refer to the scaled electron velocity and its momentum, and $\beta_{z0i} = u_{3i}/c$. Here, $\omega_{bi}^2 = (4\pi n_i e^2)/(mc^2 k_w^2)$, $\delta a = (e\delta\hat{A}\bar{z})/mc^2$, $\delta\varphi = (e\delta\hat{\theta}\bar{z})/mc^2$ and $\psi \equiv \alpha_+(\bar{z},\bar{t}) + \bar{z}$ is ponderomotive phase and $\psi_{sc}(\equiv \alpha(\bar{z},\bar{t}))$ is space-charge phase. Here, n_i, m, and e, refer to the average beam density, electron mass, value of electron charge, respectively. Ponderomotive phase and space-charge phase are given as

$$\frac{d\psi_i(\bar{z})}{d\bar{z}} = \bar{k}_+(\bar{z}) + 1 - \frac{\bar{\omega}}{\beta_{3i}} \tag{7a}$$

$$\frac{d\psi_{sci}(\bar{z})}{d\bar{z}} = \bar{k}(\bar{z}) - \frac{\bar{\omega}}{\beta_{3i}}. \tag{7b}$$

In the right-hand side of Eqs. (6b-d) the coupling of the two REBs is seen. Here $i = 1, 2$ refers to the two electron beam quantities. It is convenient to normalize all quantities to c (speed of light in vacuum) and k_w. Where Γ_+ defines the growth rate (i.e. the logarithmic derivative) of the vector potential. The averaging operator $\langle(\cdots)\rangle = (1/2\pi)\int_{-\pi}^{\pi}\sigma(\psi_0)d\psi_0(\cdots)$ is defined over an ensemble of beam electrons injected into the interaction region within one wave period. In the above differential equations, we have changed the integration parameter from $\bar{t}$ to $\bar{z}$, according to the relation $d/d\bar{t} = \beta_3(d/d\bar{z})$ (which $\beta_3 = v_3/c$).

The water-bag phase distribution function of REBs read [27],

$$\begin{cases} \frac{2\pi}{\psi_{wi}}, & \text{if } 0 \le \psi_{0i} \le \psi_{wi} \\ 0, & \text{otherwise.} \end{cases} \tag{8}$$

Here ψ_{wi} is determined the width of the i^{th} bunching REB in the initial phase. To form the pre-bunched electron beams the nonlinear evolution of the ensembles of electrons with lower energy is considered to be initially distributed uniformly at the phase region of $-\pi \le \psi_0 \le 0$. Here, $\sigma(\psi_0)$ refers to the initial beam distribution in phase. Since it is assumed that the REBs have bunched, so, it has taken as $\sigma(\psi_0) = 1$ at the phase region of $-\pi \le \psi_0 \le 0$, and $\sigma(\psi_0) = 0$ at the phase region of $0 \le \psi_0 \le \pi$. Where, $\psi_0(= -\bar{\omega}\bar{t}_0)$ is the initial phase, which $\bar{t}_0$ is normalized injection time. The particles that enter the interaction region of the wiggler at time $\bar{t}_0$ separated by integral multiples of the wave period will have identical orbits.

In the case of a steady-state amplifier configuration, we could integrate in z and write the Lorentz force equations in the form [12, 30, 31],

$$\frac{du_{1i}}{d\bar{z}} = u_{2i} + [\delta a(\frac{\omega}{v_{3i}} - k_+)\sin\psi_i + \frac{d\delta a}{d\bar{z}}\cos\psi_i], \tag{9a}$$

$$\frac{du_{2i}}{d\bar{z}} = -u_{1i} + [\delta a(\frac{\omega}{v_{3i}} - k_+)\cos\psi_i - \frac{d\delta a}{d\bar{z}}\sin\psi_i], \tag{9b}$$

$$\begin{aligned} \frac{du_{3i}}{d\bar{z}} = k_+\delta a\frac{u_{1i}\sin\psi_i + u_{2i}\cos\psi_i}{u_{3i}} - \\ \frac{1}{\beta_{3i}}(k\delta\varphi_i\sin\psi_{sci} - \frac{d}{d\bar{z}}\delta\varphi_i\cos\psi_{sci}) + \\ \hat{\Omega}_w\frac{u_{2i}}{u_{3i}} - \frac{d\delta a}{d\bar{z}}\frac{u_{1i}\cos\psi_i - u_{2i}\sin\psi_i}{u_{3i}}. \end{aligned} \tag{9c}$$

Here, $\hat{\Omega}_w = (eB_w)/(mc^2k_w)$ and it has been assumed that the amplitudes and phases are slowly varying functions of the position, i.e.$|\partial\delta a/\partial z| \ll |k_+\delta a|$, and this occurs only in the vicinity of the wave-particle resonance at $\omega \approx (k_+ + k_w)u_3$.

Equations (6-9) give a set of 10N+4 self-consistent first-order nonlinear differential equations which describe the wave evolution in a two-stream FEL. Here, N refers to the total number of electrons subjected to the initial conditions. The set of coupled differential Eqs. (6-9) has been solved numerically for a two-stream FEL, which has worked in a seeded amplifier mode. Two electron beams are assumed in the form of a squared distribution function that peaked around $\gamma_{01} = 4$ and $\gamma_{02} = 4.5$, without any energy spread. The transverse displacement and the velocity of the electron beam at the entry plane are taken to be zero. The electromagnetic mode was chosen to correspond to the highest linear growth rate, which is determined from the intersection of the slow space-charge wave mode and the transverse electromagnetic mode [25]. One of two resonance frequencies (ω, k_+) of arbitrary amplitude which is extracted from dispersion relation is injected into the system in concert with two relativistic, mono-energetic, and noiseless electron beams. Here, the scaled amplitude of the seed wave is considered as $\delta\bar{a}$=1.0×10^{-6}.

3. Numerical solution

The set of coupled differential Eqs. (6, 7, and 9), has been solved numerically for a two-stream FEL working in an amplifier mode. The typical parameters of the two-stream FEL system used in this work are the common ones for the numerical analyses, which are listed in Table 1.

The average of the variables in the dynamical equations have been calculated by Simpson's rule. The electron beams are bunched, so they are distributed uniformly in phase at the region of $-\pi \le \psi_0 \le 0$. Since the wiggler field increases adiabatically from zero at the entry plane, the growth rate of the vector potential is initially zero as well (i.e.$(\Gamma_+)_0 = 0$). As seen in Fig. 1, while both distributions of the REBs is the same, the scaled amplitude (which corresponds to the peak output power) is lower than in the comparison to the case in which the distribution of the REBs is different from each other. When unmodulated REBs are fed to the entrance of the wiggler the maximum scaled amplitude for the non-bunched REBs (blue curve) is about 5.411×10^{-4} ($-\pi \le \psi_0 \le \pi$, $\psi_w = 2\pi$). In this situation the scaled axial distance is about 123.2, while the maximum scaled amplitude for the bunched REBs is about 5.854×10^{-4} and its scaled axial distance is about 117.7 (dashed curve); maximum scale amplitude increases by about 8.18%. Let us consider just one REB as a bunched beam, such cases are plotted in Fig. 1.

As seen from Fig. 1, when we consider one REB distributed uniform in phase $0 \le \psi_0 \le 2\pi$ and the other one distributed in phase $0 \le \psi_0 \le \pi/2$, the maximum the scaled amplitude for this case (black curve) is 1.674×10^{-3} and it's scaled axial distance is about 124.8. The saturation length decreased by about $7-2\%$. However, its maximum scaled amplitude has an increasing about 209.3%. This effect is reasonable, in the case of using unmodulated electron beams the ponderomotive potential is formed by beating the magnetic wiggler field and seed EMW, which consequently REMs

Table 1. 1D simulation parameters for the model of two stream FEL under consideration.

Parameter	Value
Maximum magnetic field (B_w)	2.41 kG
Wiggler period (λ_w)	2 cm
Relativistic parameters	4 and 4.5
FEL constant	0.5
Number of macroparticles	21

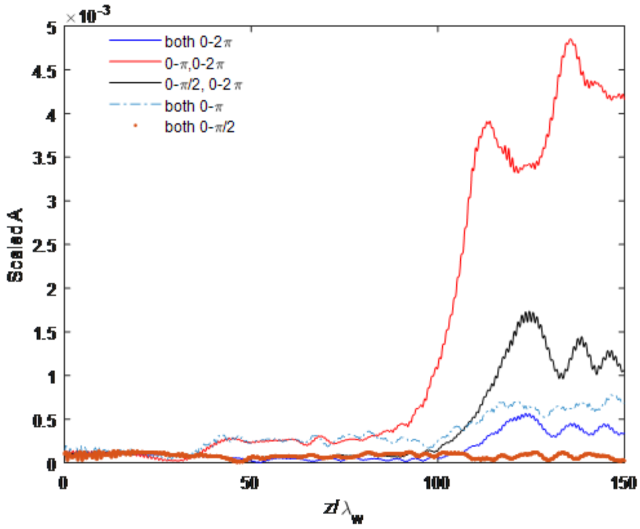

Figure 1. Graphs of the scaled amplitude of the radiation field versus scaled axial for the case of different distribution in the phase of REBs; $0 \leq \psi_0 \leq 2\pi$(blue),$0 \leq \psi_1 \leq \pi$, $0 \leq \psi_2 \leq 2\pi$(red), $0 \leq \psi_1 \leq \pi/2$, $0 \leq \psi_2 \leq 2\pi$(black), $0 \leq \psi_{1,2} \leq \pi$ (dashed-blue), $0 \leq \psi_{1,2} \leq 2\pi$ (dashed-red), other parameters are fixed and are listed in Table 1.

become bunched after several wiggler periods. However, using a pre-bunched REBs, this bunching has been provided at the entrance of the wiggler. Thereby, the shortcoming of the wiggler periods to saturation length and augmenting of the output power results. When the bunching band of REB (the REB with lower energy) is at the region phase of $0 \leq \psi_0 \leq \pi$ (red curve in Fig. 1), two peaks at saturation profile appear, and a jump is created in the normalized amplitude (the first peak is about 3.912×10^{-3}). In addition, the saturation length is also reduced (it is located at 2.28 m). When a pre-bunched beam is injected into the interaction region by using a single-stage or two-stage pre-buncher, the fraction of trapped particles in the ponderomotive wave will be increased [9–11]. These results are in well agree with the outcome of Ref. [27]. Here, a 1D simulation code is developed to analyze the two-stream FEL with a helical wiggler. Developing the simulation code to cover the tapered wiggler along with an axial magnetic field, using FERMI Elettra synchrotron radiation parameters, and comparing the results with the GINGER simulator is our future work.

4. Conclusion

In this manuscript, a 1D simulation code is developed to analyze the two-stream FEL with a helical wiggler. The effect of pre-bunching of the relativistic electron beams on the performance of the free electron laser with two-stream has been verified. It was found that by using a pre-bunched REB (the REB with lower energy), saturation length has been decreased by about 7.2%. However, its maximum amplitude more affected, so that, it was increased by about 209.3%.

Acknowledgements
Many thanks to the research chancellor of Mashhad and Sabzevar Branches, Islamic Azad University.

Authors Contributions
All the authors have participated equaly in the intellectual content, conception, calculations, analysing and interpretation of the data (when applicable), as well as writing of the manuscript.

Availability of data and materials
Data presented in the manuscript are available via request.

Conflict of Interests
The author declare that they have no known competing financial interests or personal relationships that could have appeared to influence the work reported in this paper.

References

[1] E. L. Saldin, E. A. Schneidmiller, and M. V. Yurkov. “The Physics of Free Electron Lasers. ”. *Springer-Verlag*, , 2000.

[2] S. Kumar, Sh. Thakur, and V. Vij. “Resonant terahertz generation by the interaction of laser beams with magnetized anharmonic carbon nanotube array.”. *Plasmonics*, **17**, 2021. DOI: https://doi.org/10.1007/s11468-021-01529-z.

[3] S. Kumar, N. Kant, and V. Thakur. “THz generation by self-focused Gaussian laser beam in the array of anharmonic VA-CNTs.”. *Optical and Quantum Electronics*, **55**, 2023. DOI: https://doi.org/10.1007/s11082-023-04562-w.

[4] S. Kumar, Sh. Kant, N. Vij, and V. Thakur. “Resonant terahertz generation by cross-focusing of Gaussian laser beams in the array of vertically aligned anharmonic and magnetized CNTs.”. *Optics Communications*, **513**, 2022. DOI: https://doi.org/10.1016/joptcom.128112.

[5] S. Kumar, V. Thakur, and N. Kant. “Magnetically enhanced THz generation by self-focusing laser in VA-MCNTs.”. *Physica Scripta*, **98**, 2023. DOI: https://doi.org/10.1088/1402-4896/ace1ae.

[6] S. Kumar, N. Kant, and V. Thakur. “Magnetically tuned THz radiation through the HA-HA-CNTs under the effect of a transverse electric field.”. *Indian Journal of Physics*, **98**, 2023. DOI: https://doi.org/10.1007/s12648-023-02849-y.

[7] V. Thakur, N. Kant, and S. Kumar. “THz Field Enhancement under the Influence of Cross-focused Laser Beams in the m-CNTs.”. *Trends in Sciences*, **20**, 2023. DOI: https://doi.org/10.48048/tis.2023.5284.

[8] V. Thakur and S. Kumar. “Terahertz generation in ripple density hot plasma under the influence of static magnetic field. ”. *Journal of Optics*, , 2024. DOI: https://doi.org/10.1007/s12596-023-01588-x.

[9] Z. Rezaei and B. Farokhi. “Start current and growth rate in Smith–Purcell free-electron laser with dielectric-loaded cylindrical grating. ”. *Journal of Theoretical and Applied Physics*, **14**, 2020. DOI: https://doi.org/10.1007/S40094-019-00358-0.

[10] T. Mohsenpour. “Steady-state electron trajectories in a free electron laser with ion-channel and axial magnetic field in the presence of self-fields.”. *Journal of Theoretical and Applied Physics*, **8**, 2014. DOI: https://doi.org/10.1007/S40094-014-0128-6.

[11] S. Meydanloo and S. Saviz. “Dispersion relation and growth rate in two-stream thermal plasma-loaded free-electron laser with helical wiggler. ”. *Journal of Theoretical and Applied Physics*, **9**, 2015. DOI: https://doi.org/10.1007/s40094-014-0158-0.

[12] E. Allaria, P. Cinquegrana, S. Cleva, D. Cocco, M. Cornacchia, P. Craievich, I. Cudin, G. D’Auria, et al. “Highly coherent and stable pulses from the FERMI seeded free-electron laser in the extreme ultraviolet. ”. *Nature Photonics*, **6**, 2012. DOI: https://doi.org/10.1038/NPHOTON.2012.233.

[13] E. Allaria, D. Castronovo, P. Cinquegrana, P. Craievich, M. Dal Forno, M. B. Danailov, G. D’Auria, A. Demidovich, et al. “Two-stage seeded soft-X-ray free-electron laser. ”. *Nature Photonics*, **7**, 2013. DOI: https://doi.org/10.1038/NPHOTON.2013.277.

[14] P. R. Ribic, A. Abrami, L. Badano, M. Bossi, H-H Braun, N. Bruchon, F. Capotondi, D. Castronovo, et al. “Coherent soft X-ray pulses from an echo-enabled harmonic generation free-electron laser.”. *Nature Photonics*, **13**, 2019. DOI: https://doi.org/10.1038//s41566-019-0427-1.

[15] H. P. Freund. “Nonlinear analysis of free-electron-laser amplifiers with axial guide fields.”. *Physical Review A*, **27**, 1983. DOI: https://doi.org/10.1103/PhysRevA.27.1977.

[16] Jr. H. P. Freund and T. M. Antonsen. “Principles of Free Electron Laser.”. *Chapman & Hall, London*, , 1996.

[17] B. W. J. McNeil, G. R. M. Robb, and M. W. Poole. “Two-beam free-electron laser. ”. *Physical Review E*, **70**, 2004. DOI: https://doi.org/10.1103/PhysRevE.70.035501.

[18] I. Ben-Zvi, K. M. Yang, and L. H. Yu. “The “fresh-bunch” technique in FELS. ”. *Nuclear Instruments and Methods in Physics Research Section A Accelerators Spectrometers Detectors and Associated Equipment*, **318**:62–72, 1992. DOI: https://doi.org/10.1016/0168-9002(92)91147-2.

[19] C. Emma, N. Sudar, P. Musumeci, A. Urbanowicz, and C. Pellegrini. “High efficiency tapered free-electron lasers with a prebunched electron beam.”. *Physical Review Accelerator and Beams*, **20**, 2017. DOI: https://doi.org/10.1103/PhysRevAccelBeams.20.110701.

[20] N. Sudar, P. Musumeci, J. Duris, I. Gadjev, M. Polyanskiy, I. Pogorelsky, M. Fedurin, C. Swinson, K. Kusche, M. Babzien, et al. “High efficiency energy extraction from a relativistic electron beam in a strongly tapered wiggler.”. *Physical Review Letters*, **117**, 2016. DOI: https://doi.org/10.1103/PhysRevLett.117.174801.

[21] E. Noori, N. Aral, M. H. Rouhani, and M. Sharifzadeh. “Effect of beam pre-bunching on saturation characteristics of Raman free electron laser with helical wiggler and axial magnetic field. ”. *Results in Physics*, **12**, 2019. DOI: https://doi.org/10.1016/j.rinp.2018.12.075.

[22] A. Bhasin and S. Sharma. "Effect of beam prebunching on gain and efficiency in a free electron laser: Nonlocal theory.". *Physics of Plasmas*, **14**, 2007. DOI: https://doi.org/10.1063/1.2751602.

[23] F. Bazouband and E. Mir. "Simulation of pre-bunched free electron laser oscillator in the THz regime.". *Iranian Journal of Physics Research*, **20**, 2020. DOI: https://doi.org/10.47176/ijpr.20.2.25731.

[24] E. G. Bessonov. "Method of electron bunching. ". *Nuclear Instruments and Methods in Physics Research Section A Accelerators Spectrometers Detectors and Associated Equipment*, **528**, 2004. DOI: https://doi.org/10.1016/j.nima.2004.04.091.

[25] G. Bekefi and K. D. Jacobs. "Two-stream, free-electron lasers.". *Journal of Applied Physics*, **53**, 1982. DOI: https://doi.org/10.1063/1.331278.

[26] M. Botton and A. Ron. "Gain enhancement in a free electron laser by two-stream instability.". *Journal of Applied Physics*, **67**, 1990. DOI: https://doi.org/10.1063/1.345091.

[27] W. Liu, Z. Yang, and Z. Liang. "Instability of two-stream free-electron laser with an axial guiding magnetic field.". *International Journal of Infrared and Millimetre Waves*, **27**, 2006. DOI: https://doi.org/10.1007/s10762-006-9095-6.

[28] F. M. Aghamir and N. Mahdizadeh. "Effects of beam temperature and density variation on the growth rate of a two-stream free electron laser. ". *Physics of Plasmas*, **19**, 2012. DOI: https://doi.org/10.1063/1.3694732.

[29] V. V. Kulish, A. V. Lysenko, and V. I. Savchenko. "Two-stream free electron laser, General properties. ". *International Journal of Infrared and Millimetre Waves*, **24**, 2003. DOI: https://doi.org/10.1023/A:1021838618554.

[30] N. Mirian and B. Maraghechi. "Thermal effect on prebunched two-beam free electron laser.". *Physics of Plasmas*, **20**, 2013. DOI: https://doi.org/10.1063/1.4817025.

[31] N. Mahdizadeh and F. M. Aghamir. "Effect of two-stream instability on the saturation mechanism of a two-stream free electron laser with a helical wiggler pump. ". *Nuclear Instruments and Methods in Physics Research Section A Accelerators Spectrometers Detectors and Associated Equipment*, **688**, 2012. DOI: https://doi.org/10.1016/j.nima.2012.04.020.